HHS Public Access

Author manuscript

Emerg Contam. Author manuscript; available in PMC 2025 April 24.

Published in final edited form as:

Emerg Contam. 2024 December ; 10(4): . doi:10.1016/j.emcon.2024.100390.

Application and efficacy of beidellite clay for the adsorption and detoxification of deoxynivalenol (vomitoxin)

Johnson O. Oladele,

Meichen Wang,

Kelly J. Rivenbark,

Timothy D. Phillips*

Department of Veterinary Physiology and Pharmacology, College of Veterinary Medicine & Biomedical Sciences, Texas A&M University, College Station, TX, USA

Abstract

The incidence of mycotoxin occurrence throughout the entire lifespan of some agricultural products could be due to climatic conditions and environmental factors (including high temperature, drought, and heavy rainfall) that enhance growth of fungi. Deoxynivalenol (DON) which is also referred to as vomitoxin is a mycotoxin produced from many Fusarium species. DON ranks high among the prominent mycotoxins in cereal products and is a ubiquitous toxin in livestock feeds. DON's adverse effects present major health challenges in both livestock and humans. The use of natural sorbents including smectite clays, is an economically feasible strategy to mitigate mycotoxin toxicities. Previous studies have demonstrated the potential of edible clays as protective components of human food and animal feed to alleviate toxicity associated with short-term exposure to mycotoxins including DON. Hence, this study was designed to investigate the sorption mechanisms of DON onto the binding surfaces of beidellite clay, assessing essential binding parameters such as enthalpy, free energy, binding capacity, affinity, and plateau surface density. These markers were used to predict availability of DON under the experimental conditions. Furthermore, the protection of beidellite clay against DON-induced toxicity was carried out using living organisms susceptible to DON toxicity, including *Hydra vulgaris* and *Lemna minor*. These studies investigated the dose-dependent detoxification of DON by 0.05–2 % inclusion of beidellite. Beidellite exhibited more than 75 % protection in *Lemna minor* and 53 % in *Hydra vulgaris* validating that this clay is effective in detoxifying DON. During emergencies,

*Corresponding author. tphillips@cvm.tamu.edu (T.D. Phillips).

CRediT authorship contribution statement

Johnson O. Oladele: Writing – review & editing, Writing – original draft, Investigation, Formal analysis, Data curation. **Meichen Wang:** Writing – review & editing, Writing – original draft, Investigation, Formal analysis, Data curation. **Kelly J. Rivenbark:** Investigation, Data curation. **Timothy D. Phillips:** Writing – review & editing, Writing – original draft, Supervision, Project administration, Funding acquisition, Conceptualization.

Declaration of competing interest

The authors declare that they have no known competing financial interests or personal relationships that could have appeared to influence the work reported in this paper.

Appendix A. Supplementary data

Supplementary data to this article can be found online at https://doi.org/10.1016/j.emcon.2024.100390.

or after disasters, inclusion of edible clay like beidellite in food, water or capsules could reduce bioavailability of DON and halt potential exposures to humans and animals.

Keywords

Mycotoxins; Deoxynivalenol; Vomitoxin; Adsorbent; Beidellite clay; Thermodynamics; Kinetics; Isotherms

1. Introduction

The presence of naturally occurring toxins poses major health threats to both human and animal health. Mycotoxins are predominant among these toxins during drought. Pollution of agricultural products and food and feed by mycotoxins results in significant consequences such as loss of agricultural products, and diverse health complications ranging from acute to lethal effects in humans and animals [1]. The World Health Organization (WHO) and the International Agency for Research on Cancer (IARC) highlighted the deleterious effect of mycotoxin-mediated toxicities on socio-economical development and health of developing countries [2]. About 500 million individuals in these nations of the world are affected directly or indirectly by mycotoxins exposure on a daily basis [3]. A recent evaluation of mycotoxin presence in food items revealed that the concentration of deoxynivalenol (DON) is higher than the recommended threshold in a majority of the assessed samples [4].

DON, which is also known as vomitoxin is a member of the epoxy-sesquiterpenoid and type B trichothecene family. It is produced by *Fusarium graninearm*. and has been isolated, purified and characterized from moldy barley grains [5]. DON displays solubility in ethanol, acetonitrile, water and other polar solvents, exhibiting stability even at increased temperatures and low pH levels. Previous investigations have documented that wheat polluted with DON maintains a deleterious effect for up to four years of storage [6]. In spite of concerted efforts to eradicate these toxins in food items and agricultural produce, complete removal remains elusive because DON is heat-stable and can affect food items or farm products at any stage of production. As there are often several potential sources of fungal infection, preventative measures against mycotoxin and fungal contamination need to be implemented at an integrated level throughout the entire food production chain (plant growth, harvest, storage, and distribution). Potential strategies to mitigate the toxicity of mycotoxins encompass chemical, physical and biological detoxification approaches, with new inventions in nutritional strategies evolving as a potential approach.

DON is stable and can be involved in every stage of the food chain prior to consumption [7]. Based on the worldwide evaluation of more than 21,000 maize and wheat samples, DON was the most common mycotoxin. The investigation reported high levels of DON pollution in feed samples (i.e. 76 %, 78 % and 86 %) in areas like Central America, the Middle East, and mainland China and Taiwan, respectively [8]. The limits for DON in grains varied across countries due to their individual differences. The United States Food and Drug Administration has established a safety level of 1 mg/kg in food, with a precise limit for wheat and its varieties at 4 mg/kg [9]. China’s national standard limit (GB2761-2017) for DON in grain and its varieties was set at 1 mg/kg [10]. Nevertheless, the toxic effects of this

toxin are associated with a number of health threatening conditions such as haemorrhage, immunosuppression, digestive disorder, and vomiting. Thus, there is a critical need for an effective approach to mitigate the toxic effects of DON.

The use of viable and suitable sorbents for the adsorption of toxins is one of the well-established approaches for the neutralization and elimination of mycotoxins [11–14]. One vital industrial principal technique for waste management is adsorption. A solid substance known as the adsorbent is utilized in an intricate physicochemical procedure to selectively remove solute materials from the aqueous solution using attractive forces to accumulate solute materials onto its surface and interfacial boundaries. In order to decrease mycotoxin adsorption from the gut and create interactions with the molecules in the gastrointestinal tract, adsorbents function as sequestrants. This lowers the systemic toxicity in both humans and animals [15,16].

Organic adsorbents such are yeast cell wall (YCW) have been reported to demonstrate sorption capacity for DON [17]. The primary components of YCW are lipids, proteins, and polysaccharides, together with glucans and mannans. It has been shown that mannans (derived from *S. cerevisiae*) are capable of binding DON at various pH levels; the rate of adsorption decreases as the concentration of DON increases [18]. YCW displays a wide range of mycotoxin adsorption loci and distinct binding processes, including hydrophobic or ionic interactions and hydrogen bonds [19]. When micronized fibers and biosorbents, like pectin- and fiber-rich apple pomace, were added to DON-contaminated feed and evaluated in pigs as mycotoxin adsorbents, the report indicated that the harmful effects of DON could be mitigated [20]. Other sorbents that have been used to remove DON include active carbon [21], alginate/carboxymethyl cellulose sodium composite loaded with calcium (SA/CMC-Ca) [22], montmorillonite [23], modified hydrated sodium calcium aluminosilicate (HSCAS) [24]. Although activated carbon is a highly effective adsorbent, its limitations include variations in performance dependent on their source, activation methods and formation of dark coloration that could affect the appearance of the food [25].

Previous studies have elucidated montmorillonite clays as being among the most economical and effective adsorbents for the removal of toxins [12–14]. Clays are classified as finely grained minerals (less than 2-μm fraction of soil) with inherent plasticity which can solidify through desiccation or calcination while retaining optimum moisture content. Most of these clays comprise phyllosilicate and other components, which may offer rigidity or plastic qualities when they are dried or baked [26]. The fine-grained, negatively charged silicate mineral structure of the clays is the basis of their adsorptive abilities. This electrostatic charge can be effectively neutralized by the adsorption of suitable molecules especially the cations. Furthermore, clays have relatively large surface areas with values up to 800 m^2/g, which can greatly enhance their adsorption capabilities [27].

Smectite clays are types of non-metallic minerals composed principally of hydrated sodium calcium aluminum silicate. These minerals are members of the monoclinic clay and are often replaced by potassium, iron, and other cations, nevertheless, the precise ratio of their substituents differ due to their different sources. Beidellite, named from Beidell, Colorado, USA is a dioctahedral smectite. It is a member of the dioctahedral smectite group with a

typical general formula: $(Ca_{0.5}, Na)_{0.3}Al_2(Si, Al)_4O_{10}(OH)_2.nH_2O$. It has been demonstrated that beidellite and montmorillonite clays are beneficial in the detoxification of ochratoxin A, aflatoxins, fumonisin B_1, and zearalenone in food and feed materials [28,29]. However, there is no available report on the efficacy of beidellite for the mitigation of vomitoxin, hence the purpose of this study. Based on the aforementioned, this study investigated the sorption mechanisms of DON onto the surfaces of beidellite by determining binding parameters including binding capacity, affinity, plateau surface density, enthalpy and free energy. Furthermore, the detoxification efficacy of beidellite was elucidated using DON-sensitive living organisms, *Hydra vulgaris* and *Lemna minor*.

2. Materials and methods

2.1. Clay material and chemicals

Beidellite clay (SBCa-1) with chemical composition $(Ca_{0.5}, Na)_{0.3}Al_2(Si, Al)_4O_{10}(OH)_2.nH_2O$, containing 5 % poorly crystalline kaolinite was sourced from the University of Missouri Columbia clay mineral repository, Columbia MO. Its cation exchange capacity is 140 meg/100g [30]. Beidellite clay was collapsed by heating at 200 °C for 30 min and 800 °C for 1 h. The surface was decreased as indirect evidence indicating that heat had dehydrated and dehydroxylated the siloxane surface of the clay resulting in partial collapse of the interlayer space. Ultrapure deionized water (18.2 MΩ) was generated within the lab using an Elga automated filtration system (Woodridge, IL). High-performance liquid chromatography (HPLC)-grade acetonitrile, simulated gastric fluid, simulated intestinal fluid and pH buffers (4.0, 7.0, and 10.0) were purchased from VWR (Atlanta, GA, USA). DON (>98 % purity) was purchased from Sigma-Aldrich, St. Louis, MA.

2.2. Adsorption isotherms

DON stock solution (1250 ppm) was prepared by dissolving its pure powder in acetonitrile. Using protocols previously established in our laboratory [31,32], an appropriate amount (160 μL) of the stock solution of DON was measured using a glass syringe to prepare 2 ppm solutions of DON in 100 mL of pH 2 and pH 6 water. The choice of this concentration was based on the ideal sorbent-to-toxin ratio required to attain saturation in isotherm plots. To explore the relationship between the adsorption capacity of beidellite and DON concentrations, and estimate the effective beidellite dose, 0.03 g (4 mg/mL) of beidellite clay was introduced into a gradient of 1.5 mL DON solutions ranging from 5 % to 100 % without changing the pH of the solution. The pH of the solutions was monitored by a pH meter. Control solutions contained 1.5 mL of blank water (pH 2 and pH 6), DON and beidellite in water, respectively. To replicate the conditions of the human stomach and intestine, these solutions were shaken at pH 2 and pH 6 at 1000 rpm and 37 °C for 2 and 48 h, respectively. The times were chosen to simulate average human stomach and intestine digestion durations. Adsorption isotherms in gastrointestinal conditions were repeated using the protocol described above with simulated gastric fluid (SGF) and simulated intestinal fluid (SIF).

In the thermodynamic analyses, the mixtures comprising beidellite/DON combinations and controls were shaken at 1000 rpm at three temperatures: 4 °C, 18 °C and 37 °C to calculate the enthalpy and interaction energy denoted as Gibbs free energy. After this, DON was separated from the beidellite/DON mixtures via centrifugation at 3000*g* for 5 min. The amount of DON in the supernatants was determined using LC-MS/MS.

2.3. Adsorption kinetics

This research utilized adsorption kinetic models to evaluate the potential of beidellite to bind DON over an exposure period of 24 h. Briefly, beidellite clay (0.03 g) was mixed with 2 ppm of DON in pH 2 water at 37 °C. The mixture was agitated at 800 rpm for 24 h, and adsorption kinetics were investigated by measuring the residual DON concentration using LC-MS/MS at 30 min intervals. The study explored Elovich, pseudo-first order, and pseudo-second order models in analyzing the adsorption dynamics [33–35].

The expression for the nonlinear pseudo first-order rate equation is depicted as:

$$q_t = q_e \times [1 - \exp(-K_1 \times t)] \quad (1)$$

Where q_e and q_t denote the amounts in mg/kg of DON adsorbed onto the binding surfaces of beidellite clay at equilibrium and time t (min). The rate constant of the first order is K_1 (min^{-1}).

The expression for the nonlinear pseudo-second order rate equation is depicted as:

$$q_t = \frac{k_2 \times qe^2 \times t}{1 + qe \times k_2 \times t} \quad (2)$$

Where q_e and q_t denote the amounts in mg/kg of DON adsorbed onto the binding surfaces of beidellite clay at equilibrium and time t (min). The rate constant of the second order is K_2 (mg/kg min).

The expression for the Elovich equation is depicted as:

$$q_t = 1/b \ \ln \ ab + 1/b \ \ln \ t \quad (3)$$

This investigation entails determining the initial adsorption rate (expressed in mg/kg min) denoted as 'a' and the parameter 'b' which correlated with the extent of surface covered and activation energy engaged in chemisorption (measured in mg/kg). Computational operations were employed utilizing a trial-and-error approach to ascertain the kinetic parameters of nonlinear models. The parameters were derived by minimizing the squared deviation and the coefficient of determination between the observed experimental data and the anticipated values during computer simulations.

2.4. Analytical method

An analysis of DON was conducted utilizing a Waters Acquity® Ultra Performance Liquid Chromatograph (UPLC)-Mass Spectrometry (MS)/MS system, employing a BEH C18 column 1.7 μm (50 × 2.1 mm) [36]. The separation was accomplished through a mobile phase comprising water with 0.3 % (v/v) formic acid (eluate A) and acetonitrile with both 5 mmol/L ammonium formate and 0.3 % formic acid (eluent B), with a gradient ranging from 5 % to 100 % eluate B over a duration of 4 min, at a flow rate of 0.3 mL/min. The injection volume stood at 40 μL, with a positive electrospray ionization mode (ESI+) at a 4.5 kV spray voltage. Nitrogen gas served as both the collision and curtain gas, while argon gas was utilized as the nebulizer and heating gas. The source temperature, desolvation gas flow rate, temperature and capillary voltage were maintained at 350 °C, 600 L/h, 120 °C, and 3 kV, respectively. Operation of the mass spectrometry employed the multiple reaction monitoring (MRM) mode, with the precursor and product ions monitored at 297.3 and 203.5/249.5, respectively, using unit mass resolution in the ion mass analyzer. Control and data acquisition for the LC-MS/MS system were managed through Empower analyst software. Validation of the DON detection method involved preparing a standard solution in distilled water across concentrations ranging from 0.1 ppm to 10 ppm to construct standard curves with linearity ($r^2 > 0.999$).

2.5. Data calculations and curve fitting

On isotherm graphs, DON concentration was determined by comparing the concentration (mol/kg) between the test groups and control. The R programming language and Table-curve 2D (Systat software, Inc. Palo Alto, CA) were utilized to explore the adsorption data and derive specific parameters. The R code calculated the adsorption data and used maximum likelihood estimation to check their compliance with well-known and established models. Confidence intervals and standard errors were calculated in a procedure employing the information matric method [37,38]. Adsorption isotherms based on the mean of the observed data points and the 95 % confidence intervals from triplicate studies were shown using the Langmuir model. The Langmuir model illustrates adsorption of a monolayer on a surface with a finite number of identical sites and homogeneous adsorption energies. Adsorption sites in a perfect Langmuir scenario do have homogeneous levels of energy, indicating a large homogeneous surface with modest interactions between the adsorbed species.

$$\text{Labgmuir model} \quad q = Q_{max} \frac{K_d \, C_w}{1 + K_d \, C_w} \tag{4}$$

where C_w = equilibrium concentration of deoxynivalenol (mol/L), K_d = Langmuir distribution constant, Q_{max} = maximum binding capacity (mol/kg), and q = the amount of deoxynivalenol adsorbed (mol/kg).

To determine $Ke°$ from K_d, the following equation was used:

$$K_e° = \frac{K_d[\text{adsorbate}]°}{\gamma}$$

(5)

where $K_e°$ is the thermodynamic equilibrium constant, $[adsorbate]°$ is the standard concentration of the adsorbate = 1 mol/L, and γ is the coefficient of activity.

The enthalpy (ΔH) and free energy ($\Delta G°$) were determined by using the Gibbs free energy equation together with the adsorption parameters and van't Hoff equation as given below:

$$\Delta G = \Delta G° + RTInKe°$$

(6)

$$\Delta H = \frac{-RIn\left(\frac{K_{d2}}{K_{d1}}\right)}{\left(\frac{1}{T_2}\right)-\left(\frac{1}{T_1}\right)}$$

(7)

where T (absolute temperature) = 273 + t (°C) and R (gas constant) = 8.314 J/mol/K. When $\Delta G°$ is positive, the adsorption process is not favored and could not be significant (Ke° < 1). However, if the value is negative, it is an indication that adsorption process is enhanced thermodynamically and is proceeding forward (Ke° >1).ΔG will be zero for an adsorption system in equilibrium.

2.6. Hydra vulgaris bioassay

Hydra vulgaris is an established *in vivo* model to investigate the toxicity of mycotoxin including DON [39]. The *Hydra vulgaris* organisms used in this study were obtained from Environmental Canada in Montreal and bred at a constant temperature of 18 °C in hydra medium consisting of 147 mg/L $CaCl_2$, 115 mg/L N-tris [hydroxymethyl]methyl-2-aminoethanesulfonic acid (TES), and 4 mg/L EDTA in 18.2 MΩ water, adjusted to pH 6.9–7.0. Over the years, the morphology of Hydra has been established and used as a biomarker for the estimate of toxicity of substances using a detailed hydra classification scoring system from 0 to 10 through a dissecting microscope. This system scores 10 when the hydra is healthy with long tentacles and scores 0 when the hydra is considered dead and/or dissolved. To explore the toxicity profile of DON, hydra were exposed to varying concentrations of DON between 0 and 10 ppm. The minimum effect dose (MED) which leads to the complete mortality of the hydra colony within 92 h was recorded and used for the detoxification assessment using beidellite insertion at rates ranging from 0.05 % to 2 %. The MED (9 ppm) used for the detoxification study is within the range of EU guideline for DON [40]. The DON-beidellite complex was made using hydra media and then introduced to the hydra colonies. The experimental groups comprise three hydra colonies each in 4 mL of testing media at 18 °C. To assess the levels of toxicity of DON and protection offered by the inclusion of beidellite, average scores were documented at precise intervals (0, 4, 20, 28, 44, 68, and 92 h).

2.7. Lemna minor (duckweed) bioassay

Lemna minor has been documented for the toxicity assessment of DON [41]. *Lemna minor* was obtained from AquaHabit, England, and was cultivated under a carefully monitored environment. *Lemna minor* colonies were exposed to 16 h of light from cool white, fluorescent bulbs maintained at 400 ft-c intensity, with an average temperature of 25 °C. The growth of the plant was supported by a formulated Steinberg nutrient media using a standardized protocol containing (3.46 mM KNO_3, 1.25 mM $Ca(NO_3)_2$, 0.66 mM KH_2PO_4, 0.072 mM K_2HPO_4, 0.41 mM $MgSO_4$, 1.94 μM H_3BO_3, 0.63 μM $ZnSO_4$, 0.18 μM Na_2MoO_4, 0.91 μM $MnCl_2$, 2.81 μM $FeCl_3$, 4.03 μM EDTA; Ph 5.5 ± 0.2) [42]. Three colonies of *Lemna minor*, each with three fronds were chosen at random and placed in separated pyrex dishes. They were then incubated for 7 days with the lids of the dishes a little loose. For the toxicity investigation, the plants were subjected to various concentrations of DON ranging from 0.1 to 5 ppm. In the detoxification study, 5 ppm of DON was treated with 0.2 % beidellite clay for 7 days, and a dose-dependent detoxification assessment was carried out using varying inclusion rates of beidellite from 0.05 % to 2 %. The experiment was observed daily for changes in frond number, and surface area, using Image J software from NIH (Bethesda, MD). On the last day of the study, *Lemna minor* were homogenized in 1.5 mL of 80 % acetone to extract chlorophyll. The homogenates were incubated at −4 °C for 48 h and the amount of chlorophyll in each tube was measured at 663 nm using a UV–Vis scanning spectrophotometer (Shimadzu UV-1800, Kyoto, Japan). Growth rate and inhibitory percentage were computed using OECD guidelines [42,43].

$$\text{Growth rate} = \frac{\text{Log 10(Final frond no.)} - \text{Log 10(Initial frond no.)}}{\text{days}} \tag{8}$$

$$\text{Inhibition of growth (\%)} = 1 - \frac{\text{Frond no. in the treatment}}{\text{Frond no. in the control}} \tag{9}$$

2.8. In silico investigation of DON adsorption onto beidellite

A standard computational protocol described in earlier research was used to simulate the molecular model of beidellite clay [44,45]. ISIS Draw 2.0 (MDL information Systems, Inc., Hay Hayward, CA) was used to render the individual structure of DON and beidellite. These models were then imported into Hyperchem 8.0 (Hypercube, Inc., Gainesville, FL)). The unit cell coordinates specific to muscovite were used to build the clay model, and they were then converted into orthogonal coordinates. Setting the symmetry tasks to conform to the C2/c space group, the unit cells delineating the three-dimensional spatial structure of beidellite were constructed having the clay's d001 spacing set to 21 Å [46]. The models were subjected to energy minimization via application of the semi-empirical AM1 quantum mechanical approach. This protocol was chosen for three reasons: First, it was more accurate in simulating organic molecules than other semi-empirical techniques that were included in the software; secondly, it was known to be reliable in calculating

hydrogen bonds and it is able to represent the major framework components of beidellite including Silicon (Si), Calcium (Ca), Aluminum (Al), Magnesium (Mg), Carbon (C), Oxygen (O), and Phosphorus (P) [47,48]. To perform the *in-silico* operations that predicted the possible binding sites for the adsorption of DON onto the surface of beidellite, DON molecules were integrated into the edges, interlayer, and external basal surfaces of the clay before the system energy minimization was performed. Afterwards, techniques for depicting and recalculating hydrogen bonds were used to assess the hydrogen bond interactions. According to Hypercube [47], an atom's proximity was deemed relevant when it was less than 3.2 Å. The purpose of this iterative approach was to illustrate various binding orientations and mechanisms of the DON/beidellite interactions.

2.9. Statistical analysis

Every experiment included negative and blank control samples in this study, and they were carried out at least three times and independently replicated. One-way ANOVA was used to evaluate the statistical significance of the data and a posthoc Turkey test was used thereafter. Factors including K_d and Q_{max} derived from thermodynamics and adsorption isotherms, Lemna's frond number and surface area, together with scores from toxicity and detoxification studies of hydra were estimated for standard deviation and p-values. Bonferroni analysis was used for multiple tests and the results were considered significant at $p < 0.05$.

3. Results and discussion

3.1. Adsorption of DON onto beidellite clay at different pH

The regulatory threshold or maximum contaminant level (MCL) for DON in U.S. food items is 1 ppm. To simulate exposure exceedingly twice this level, we used DON at 2 ppm in our *in vitro* studies. At 37 °C, the adsorption isotherms depict the sorption behavior of DON onto beidellite clay in aqueous solutions with pH levels of 2 and 6, emulating stomach and intestinal conditions respectively (Fig. 1A and B). In an initial screening study, a variety of clays were included for preliminary test including calcium and sodium montmorillonites, sepiolite, polkville, zeolite, and Gibbsite clays (Supplemental Tables S1 and S2). DON showed a notably heightened affinity (K_d) of 2.28×10^6 and 2.63×10^6 with binding capacity (Q_{max}) of 0.75 mol/kg and 0.70 mol/kg at pH2 and pH6 respectively in the presence of beidellite clay (Table 2). In the simulated GI conditions, beidellite demonstrated a significant high binding capacity of 0.64 mol/kg and 0.40 mol/kg in simulated gastric fluid and simulated gastrointestinal fluid respectively. The Q_{max} in fluids with enzymes (pepsin and pancreatin in SGF and SIF respectively) is lower than pH 2 & 6 without enzymes, suggesting that enzymes could interfere with DON binding. However, the Q_{max} is still high and substantially relevant compared to our previous studies showing successful application in animal feeds as mycotoxin binders. At both simulated conditions, beidellite also showed high binding affinity of 4.23×10^6 and 9.77×10^5 at SGF and SIF conditions respectively.

This sorption aligned with the Langmuir model for beidellite, signifying a uniform and saturated binding on the clay, which is in tandem with the findings from previous studies that proposed potential high binding of DON on various clays such as smectites [49].

The notably elevated Q_{max} values across the two pH levels (pH 2 and 6) imply the superior binding capacity of beidellite clay, potentially attributed to the diverse binding site configurations. We postulate that the heightened binding stems from multiple available binding sites that accommodate DON through the establishment of hydrogen bridge bonds. Specifically, these bonds are formed between the hydroxyl terminals of DON and the unoccupied oxygen atoms within the structure of beidellite.

Furthermore, beidellite clay was subjected to a heat-induced process aimed at dehydrating and collapsing its interlayer spacing. The adsorption capacity onto the collapsed beidellite notably diminished, having a binding capacity of 0.54 mol/kg (Fig. 1C). This outcome indicated that the primary binding sites for DON predominantly exist within the interlayers, while minor binding occurs on the basal and edge site surfaces.

To ascertain the clay's maximum binding capacity at saturation (plateau surface density), we assessed the active binding sites on beidellite and compared it to the maximum binding area attained by DON, determined from isothermal analysis. The beidellite's total specific surface area has been reported to range from approximately 749 to 770 m^2/g [50], which is equivalent to 7.5×10^{22} $Å^2/g$ (using the lowest area, 749 m^2/g). Utilizing the isotherms, the calculated quantity of bound DON molecules at pH 2 was 0.73 mol/kg × 6.02×10^{23} molecules/mol, totaling 4.4×10^{20} molecules/g. With each beidellite molecule occupying a topological polar surface area of 99.5 $Å^2$, the cumulative binding area for DON is equal to $4.4 \times 10^{20} \times 99.5 = 4.4 \times 10^{22}$ $Å^2/g$, which is below the available clay surface area (7.5×10^{22} $Å^2/g$). These results imply that there is enough binding site for DON within the beidellite surface for monolayer sorption. This is consistent with the uniform site requirement for the Langmuir model and indicates a monolayer sorption process instead of a multilayer phenomenon.

3.2. Thermodynamics of adsorption of DON onto beidellite clay

Comprehending the techniques by which DON binds to beidellite surfaces and assessing the thermodynamic principles governing the interactions between DON and beidellite surfaces were essential in this study. The evaluation comprised measuring the enthalpy and binding free energy between the clay and DON at three different temperatures (4 °C, 18 °C and 37 °C) (Fig. 2). Table 1 shows that the enthalpy is −34.08 kJ/mol while the free binding energies were −35.98, −33.54, and −35.78 kJ/mol at temperatures of 4 °C, 18 °C and 37 °C respectively. This high enthalpy value is consistent with the Langmuir model of the isothermal interaction, indicating a substantial sorption of DON onto beidellite. Furthermore, the experimental results and the sorption capacity model are in tandem, indicating the importance of tight binding in propelling the DON adsorption mechanism onto beidellite.

In addition, the data presented in Table 1 demonstrates that the ΔG and ΔH parameters consistently exhibit negative values across the range of temperatures investigated within this research. These negative values signify the spontaneous and exothermic nature of the adsorption process of DON onto the beidellite clay. This implies an increase in entropy during the adsorption, suggesting the formation of inner-sphere complexes throughout the adsorption mechanism for all the composites examined [51,52].

3.3. Kinetics and equilibrium of adsorption of DON onto beidellite clay

Analyzing the dynamics and processes controlling the rate-limiting phases of adsorption behavior was the goal of the kinetics and equilibrium assessment of the adsorption process. To examine the time-dependent study, three popular kinetic models: the pseudo-first order, pseudo-second order and Elovich were used. The pseudo-second order kinetic model (Fig. 3) best characterized the adsorption of DON onto beidellite surfaces correlating the coefficient value ($r^2 \geq 0.96$) and the consistency between experimental binding capacity (qe, exp) and modeled values (qe, cal) were compared (Table 2). This finding suggested that diffusion-mediated mechanisms which are impacted by both continuous DON partitioning and heterogeneous pore size distributions, primarily determined the adsorption kinetics onto beidellite. The concentration gradient acted as the driving force for the DON adsorption onto beidellite, and the adsorption rate was directly proportional to this gradient or its square [53].

Furthermore, the kinetic data for the beidellite adsorption ability towards DON as shown in Table 1 indicated a rapid rate of adsorption. This implies that the beidellite clay porosity and adsorption could have increased. The increased charge distribution in the tetrahedral layers of beidellite in comparison to other smectite clay minerals may further strengthen the binding interaction.

The minimum addition rate of beidellite in this kinetic evaluation is consistent with the isothermal results, which showed that beidellite surfaces had a high potential for DON binding. These *in vitro* results suggest that beidellite can amplify the effectiveness of DON binding compared to other smectite clays and may be applicable as a protective strategy to reduce the bioavailability and toxicity of DON following ingestion of contaminated food.

3.4. In vitro bioassays

Validation of the *in vitro* results, safety, and efficacy of beidellite was conducted with two well-established living organism models—the hydra assay and lemna assay. DON is a potent inhibitor of protein synthesis resulting in toxicity of many organisms [54,55]. Exposure to DON within the range of 1–10 ppm exhibited severe and irreversible toxicity to hydra morphology (Fig. 4A). The toxic effect of DON also affected the feeding ability of the hydra causing 8 %, 46 %, 54 % and 100 % reduction in feeding rate based on 1, 2, 5 and 10 ppm DON treatment, respectively as depicted in Fig. 4B. This may arise from the truncated length of their tentacles which plays a crucial role in their dietary adaptation subsequent to their exposure to DON. However, the introduction of 0.05 %–2 % beidellite provided substantial (>50 %) protection to adult hydra against DON toxicity in a dose-dependent manner (Fig. 4C). The superior shielding effect of beidellite against DON aligns with the isothermal outcomes, indicating favored binding capability for DON removal.

Similarly, Fig. 5 revealed the toxicity of DON exposure at varying doses between 0.1 ppm and 5 ppm on *Lemna minor*. DON significantly impeded the growth rate of *Lemna minor* as shown by its adverse effect on chlorophyll content, surface area, and frond formation in the plant. As shown in Fig. 5D, DON induced 6 %, 11 %, 16 %, 33 % and 55 % decrease in the growth rate of *Lemna minor* exposed to 0.1, 0.5, 1, 2 and 5 ppm of DON respectively.

The negative impact of DON on plants predominantly from its capacity to impede protein synthesis [54,55]. Moreover, DON induces alterations in chlorophyll levels through various mechanisms, initially leading to a postponement of senescence during the initial phases of infection and subsequently contributing to cell bleaching and apoptosis during later stages [56]. Importantly, exposure of 0.05 %–2 % beidellite alone to *Lemna minor* did not show any sign of toxicity to Lemna (Supplemental Figs. S1A–C). Treatment with the inclusion of 2 % beidellite offered significant protection (>70 %) in the chlorophyll content of the plant (Fig. 6). Furthermore, the inclusion of varying dosages (0.05 %–2 %) of beidellite showed that the extent of protection offered by the clay increased proportionally with higher clay inclusion rates in a dose-dependent manner.

3.5. Computational assessment and molecular modeling of adsorption of DON onto beidellite clay

This study presents a molecular model depicted in Fig. 7, demonstrating the proposed interactions between beidellite clay and DON. The model highlights various binding modes of DON with binding sites on beidellite, encompassing basal surfaces, edge sites, and interlayer regions. These interactions primarily involve hydrogen bonding. Heat treatment of clay resulted in dihydroxylation of surfaces and a collapse of the interlayers, reducing the DON binding capacity by 40 % compared to parent clay. Hydrogen atoms and hydroxyl groups on DON were crucial for binding interactions, based on Hyperchem investigations. The hydrogen atoms on DON were able to engage in multiple hydrogen bonds on active surfaces of beidellite and were shown to intercalate with oxygen atoms across the negatively charged clay interlayer surfaces. These numerous hydrogen bond interactions may contribute to the observed tight binding patterns in the thermodynamic findings. These binding mechanisms conform to the Langmuir model *in vitro*, suggesting a saturable and firm attachment of DON molecule to beidellite clay surfaces, as also supported by the substantial heat of sorption. Importantly, beidellite effectively adsorbed DON at pH 2 and 6 which suggests that it will be effective at physiological pH.

4. Conclusion

DON is a very potent inhibitor of protein synthesis and represents a significant hazard to animals and humans due to its frequent occurrence in the diet. This study evaluates the efficacy of beidellite clay for the adsorption and detoxification of DON using *in vitro* analytical procedures and *in vivo* models. The findings of *in vitro* studies showed beidellite binds DON in both simulated gastric fluid and gastrointestinal fluid suggesting it is a possible enterosorbent for DON removal. Thermodynamic and kinetic analyses demonstrated the contribution of physical processes to the total adsorption and followed pseudo-second model. The *in vivo* investigation validated the *in vitro* findings indicating the inclusion of beidellite as a viable protective strategy for DON removal and detoxification. Importantly, our results indicate that beidellite exhibits the potential for safeguarding individuals and animals exposed to DON-contaminated food, feed, and water, especially during outbreaks of drought and mycotoxin emergencies.

Supplementary Material

Refer to Web version on PubMed Central for supplementary material.

Funding sources

This work was supported by funding through NIEHS P42 ES027704, and USDA Hatch 6215.

Data availability Statement

Data is available upon request.

References

[1]. Hussein HS, Brasel JM, Toxicity, metabolism, and impact of mycotoxins on humans and animals, Toxicology 167 (2001) 101–134. [PubMed: 11567776]

[2]. Weber A, Mery L, Nagy P, Polgar C, Bray F, Kenessey I, Evaluation of data quality at the Hungarian national cancer registry, 2000–2019, Cancer Epidemiology 82 (2023) 102306, 10.1016/j.canep.2022.102306. [PubMed: 36521336]

[3]. Fellone J, IARC Press Release N° 242/Comunicato Stampa N° 242 Della IARC UN NUOVO RAPPORTO DELLA IARC ESORTA AD AGIRE CONTRO LA DIFFUSA CONTAMINAZIONE DA MICOTOSSINE NEI PAESI IN VIA DI SVILUPPO Pubblicato Il 17 Febbraio 2016, France, Lyon, 2016.

[4]. Mishra S, Srivastava S, Dewangan J, Divakar A, Rath SK, Global occurrence of deoxynivalenol in food commodities and exposure risk assessment in humans in the last decade: a survey, Crit. Rev. Food Sci. Nutr 60 (1) (2019) 1–29, 10.1080/10408398.2019.1571479.

[5]. Han X, Chen L, Li W, Zhang L, Dong H, Endocytic FgEde1 regulates virulence and autophagy in Fusarium graminearum, Fungal Genet. Biol 141 (2020) 103400, 10.1016/j.fgb.2020.103400. [PubMed: 32387406]

[6]. Cao H, Wu S, Sun C, Research advancement on biosynthesis and biodegradation of Deoxynivalenol (DON), Journal of Chinese Cereals and Oils Association 28 (2013) 116–123.

[7]. Zhai Y, Zhong L, Gao H, Lu Z, Bie X, Zhao H, et al. , Detoxification of Deoxynivalenol by a mixed culture of soil bacteria with 3-epi-Deoxynivalenol as the Main intermediate, Front. Microbiol 10 (2019) 2172, 10.3389/fmicb.2019.02172. [PubMed: 31616395]

[8]. Biomin, Pesquisa Mundial de Micotoxinas: Impacto em 2021. https://www.biomin.net/br/science-hub/pesquisa-mundial-de-micotoxinas-impacto-em-2021/, 2021.

[9]. Feizollahi E, Roopesh MS, Mechanisms of deoxynivalenol (DON) degradation during different treatments: a review, Crit. Rev. Food Sci. Nutr 62 (17) (2022) 5903–5924, 10.1080/10408398.2021.1895056. [PubMed: 33729830]

[10]. China N, GB2761d2017 limit of mycotoxins in food, China (2017).

[11]. Wen J, Kong W, Hu Y, Wang J, Yang M, Multi-mycotoxins analysis in ginger and related products by UHPLC-FLR detection and LC-MS/MS confirmation, Food Control 43 (2014) 82–87.

[12]. Phillips TD, Wang M, Elmore SE, et al. , NovaSil clay for the protection of humans and animals from aflatoxins and other contaminants, Clay Clay Miner. 67 (2019) 99–110, 10.1007/s42860-019-0008-x.

[13]. Wang M, Hearon SE, Phillips TD, A high capacity bentonite clay for the sorption of aflatoxins, Food Addit. Contam 37 (2) (2020) 332–341, 10.1080/19440049.2019.1662493.

[14]. Wang M, Maki CR, Phillips TD, Development of high capacity enter-osorbents for aflatoxin B1 and other hazardous chemicals, Chem. Res. Toxicol 30 (2017) 1694–1701. [PubMed: 28768106]

[15]. Huwig A, Freimund S, Käppeli O, Dutler H, Mycotoxin detoxication of animal feed by different adsorbents, Toxicol. Lett 122 (2001) 179–188. [PubMed: 11439224]

[16]. Yiannikouris A, Andre G, Poughon L, François J, Dussap CG, Jeminet G, Bertin G, Jouany JP, Chemical and conformational study of the interactions involved in mycotoxin complexation with β-D-glucans, Biomacromolecules 7 (2006) 1147–1155. [PubMed: 16602732]

[17]. Faucet-Marquis V, Joannis-Cassan C, Hadjeba-Medjdoub K, Ballet N, Pfohl-Leszkowicz A, Development of an *in vitro* method for the prediction of mycotoxin binding on yeast-based products: case of aflatoxin B1, zearalenone and ochratoxin A, Appl. Microbiol. Biotechnol 98 (2014) 7583–7596. [PubMed: 25016345]

[18]. Cavret S, Laurent N, Videmann B, Mazallon M, Lecoeur S, Assessment of deoxynivalenol (DON) adsorbents and characterisation of their efficacy using complementary *in vitro* tests. Food Addit, Contam. 27 (2010) 43–53.

[19]. Ringot D, Lerzy B, Chaplain K, Bonhoure JP, Auclair E, Larondelle Y, *In vitro* biosorption of ochratoxin A on the yeast industry by-products: comparison of isotherm models, Bioresour. Technol 98 (2007) 1812–1821. [PubMed: 16919938]

[20]. Gutzwiller A, Czegledi L, Stoll P, Bruckner L, Effects of *Fusarium* toxins on growth, humoral immune response and internal organs in weaner pigs, and the efficacy of apple pomace as an antidote, J. Anim. Physiol. Anim. Nutr 91 (2007) 432–438.

[21]. Devreese M, Antonissen G, De Backer P, Croubels S, Efficacy of active carbon towards the absorption of deoxynivalenol in pigs, Toxins 6 (10) (2014) 2998–3004, 10.3390/toxins6102998. [PubMed: 25337799]

[22]. Shalapy A, Zhao S, Zhang C, Li Y, Geng H, Ullah S, Wang G, Huang S, Liu Y, Adsorption of deoxynivalenol (DON) from corn steep liquor (CSL) by the microsphere adsorbent SA/CMC loaded with calcium, Toxins 12 (4) (2020) 208, 10.3390/toxins12040208. [PubMed: 32218143]

[23]. Weaver AC, See MT, Hansen JA, Kim YB, De Souza ALP, Middleton TF, Kim SW, The use of feed additives to reduce the effects of aflatoxin and deoxynivalenol on pig growth, organ health and immune status during chronic exposure, Toxins 5 (2013) 1261–1281. [PubMed: 23867763]

[24]. Vila-Donat P, Marin S, Sanchis V, Ramos AJ, A review of the mycotoxin adsorbing agents, with an emphasis on their multi-binding capacity, for animal feed decontamination, Food Chem. Toxicol 114 (2018) (2018) 246–259, 10.1016/j.fct.2018.02.044. [PubMed: 29476792]

[25]. Sabater-Vilar M, Malekinejad H, Selman MHJ, Doelen MAM, Fink-Gremmels J, In vitro assessment of adsorbents aiming to prevent deoxynivalenol and zearalenone mycotoxicoses, Mycopathologia 163 (2007) 81–90. [PubMed: 17294292]

[26]. Murray HH, Applied clay mineralogy: occurrences, processing and applications of kaolins, in: Bentonites, Palygorskitesepiolite, and Common Clays, Elsevier, 2006.

[27]. Chaari I, Medhioub M, Jamoussi F, Use of clay to remove heavy metals from Jebel Chakir landfill leachate, J. Appl. Sci. Environ. Sanit 6 (2011) 143–148.

[28]. Mao J, Zhou Y, Lv G, Zhou R, Simultaneous detoxification of aflatoxin B1, zearalenone and deoxynivalenol by modified montmorillonites, Molecules 27 (1) (2022 Jan 5) 315, 10.3390/molecules27010315. [PubMed: 35011560]

[29]. Greco D, D'Ascanio V, Abbaciano M, Santovito E, Garbetta A, Logrieco AF, Avantaggiat G, Simultaneous removal of mycotoxins by a new feed additive containing a tri-octahedral smectite mixed with lignocellulose, Toxins 14 (2022) 393. [PubMed: 35737054]

[30]. Swoboda AR, Kunze GW, Reactivity of montmorillonite surfaces with weak organic bases, Soil Sci. Soc. Am. J 32 (6) (1968) 806–811, 10.2136/sssaj1968.03615995003200060029x.

[31]. Sylvia VL, Phillips TD, Clement BA, Green JL, Determination of deoxynivalenol (vomitoxin) by high-performance liquid chromatography with electrochemical detection, J. Chromatogr. A 362 (1986) 79–85.

[32]. Grant PG, Phillips TD, Isothermal adsorption of aflatoxin B (1) on HSCAS clay, J. Agric. Food Chem 46 (1998) 599–605. [PubMed: 10554284]

[33]. Tran HN, You SJ, Hosseini-Bandegharaei A, Chao HP, Mistakes and inconsistencies regarding adsorption of contaminants from aqueous solutions: a critical review, Water Res. 120 (2017) 88–116. [PubMed: 28478298]

[34]. Yuvaraja G, Prasad C, Vijaya Y, Subbaiah MV, Application of ZnO nanorods as an adsorbent material for the removal of as (III) from aqueous solution: kinetics, isotherms and thermodynamic studies, Int. J. Integrated Care 9 (2018) 17–25.

[35]. Wang M, Phillips TD, Green-engineered barrier creams with montmorillonite-chlorophyll clays as adsorbents for benzene, toluene, and xylene separations, Separations 10 (4) (2023), 10.3390/separations10040237.

[36]. Rehder Silinski MA, Gilliam JA, Fernando RA, Robinson VG, Germolec D, Cunny H, Huang MC, Furr J, Waidyanatha S, Development of an analytical method for quantitation of deoxynivalenol by UPLC-MS-MS: a preliminary assessment of gestational and lactational transfer in rats, J. Anal. Toxicol 45 (6) (2021 Jul 10) 566–572, 10.1093/jat/bkaa119. [PubMed: 32886793]

[37]. Yan F, Chu YY, Zhang K, Zhang FF, Bhandari N, Ruan GD, Dai ZY, Liu Y, Zhang Z, Kan AT, et al. , Determination of adsorption isotherm parameters with correlated errors by measurement error models, Chem. Eng. J 281 (2015) 921–930.

[38]. Gong J, Rshiny. https://jgong9.shinyapps.io/chemistry_app/, 2020.

[39]. Eagles EJ, Benstead R, MacDonald S, Handy RD, Hutchinson TH, Environmental risks to freshwater organisms from the mycotoxins deoxynivalenol and zearalenone using Species Sensitivity Distributions, Chemosphere 267 (2021) 129279, 10.1016/j.chemosphere.2020.129279. [PubMed: 33352371]

[40]. EC, (European Commission). Commission recommandation of 17 August 2006 on the presence of deoxynivalenol, zearalenone, ochratoxin A, T-2 and HT-2 and fumonisins in products intended for animal feeding. Available online: http://eur-lex.europa.eu/legal-content/EN/TXT/PDF/?uri=CELEX:32006H0576&from=EN (accessed on 30 November 2015).

[41]. Vanhoutte I, De Mets L, De Boevre M, Uka V, Di Mavungu JD, De Saeger S, De Gelder L, Audenaert K, Microbial detoxification of deoxynivalenol (DON), assessed via a lemna minor L. Bioassay, through biotransformation to 3-epi-DON and 3-epi-DOM-1, Toxins 9 (2) (2017 Feb 13) 63, 10.3390/toxins9020063. [PubMed: 28208799]

[42]. Drost W, Matzke M, Backhaus T, Heavy metal toxicity to lemna minor: studies on the time dependence of growth inhibition and the recovery after exposure, Chemosphere 67 (2007) 36–43. [PubMed: 17157350]

[43]. United States Environmental Protection Agency (EPA), OECD guidelines for the testing of chemicals 221, in: Lemna Sp, Growth Inhibition Test, Washington, DC, USA, 2006.

[44]. Teich-McGoldrick SL, Greathouse JA, Jove-Colon CF, Cygan RT, Swelling properties of montmorillonite and beidellite clay minerals from molecular simulation: comparison of temperature, interlayer cation, and charge location effects, J. Phys. Chem. C 119 (36) (2015) 20880–20891.

[45]. Teppen BJ, Rasmussen K, Bertsch PM, Miller DM, Schafer L, Molecular dynamics modeling of clay minerals. 1. Gibbsite, kaolinite, pyrophyllite, and beidellite, J. Phys. Chem. B 101 (9) (1997) 1579–1587.

[46]. Orr AA, He SJ, Wang M, Goodall A, Hearon SE, Phillips TD, Tamamis P, Insights into the interactions of bisphenol and phthalate compounds with unamended and carnitine-amended montmorillonite clays, Comput. Chem. Eng 143 (2020) 107063, 10.1016/j.compchemeng.2020.107063. [PubMed: 33122868]

[47]. Hypercube, Hyperchem release 7.0 for windows: reference manual, in: Hypercube Lnc, Ont, Waterloo, 2002. http://www.chemistry-software.com/pdf/Hyperchem_full_manual.pdf.

[48]. Gupta VP, 4-approximate Molecular Orbital Theories. Principles and Applications of Quantum Chemistry 127–153, 2016.

[49]. Zhang Q, Zhang Y, Liu S, Wu Y, Zhou Q, Zhang Y, Zheng X, Han Y, Xie C, Liu N, Adsorption of deoxynivalenol by pillared montmorillonite, Food Chem. 343 (2021) 128391, 10.1016/j.foodchem.2020.128391. [PubMed: 33268181]

[50]. Srodon J, McCarty DK, Surface area and layer charge of smectite from CEC and EGME/H_2O-retention measurements, Clay Clay Miner. 56 (No. 2) (2008) 155–174.

[51]. Ozer A, Akkaya G, Turabik M, The biosorption of acid red 337 and acid blue 324 on Enteromorpha prolifera: the application of nonlinear regression analysis to dye biosorption, Chem. Eng. J 112 (2005) 181–190.

[52]. Xiao M, Guo J, Zhao S, Li S, Adsorption of as(V) at humic acid-kaolinite-bacteria interfaces: kinetics, thermodynamics, and mechanisms, Agronomy 13 (2) (2023) 611, 10.3390/agronomy13020611.

[53]. Dankova Z, Mockovciakova A, Dolinska S, Influence of ultrasound irradiation on cadmium cations adsorption by montmorillonite, Desalination Water Treat. 52 (2014) 5462–5469.

[54]. Casale WL, Hart LP, Inhibition of 3H-leucine incorporation by trichothecene mycotoxins in maize and wheat tissue, Phytopathology 78 (1988) 1673–1677.

[55]. Rocha O, Ansari K, Doohan FM, Effects of trichothecene mycotoxins on eukaryotic cells: a review, Food Addit. Contam 22 (2005) 369–378. [PubMed: 16019807]

[56]. Bushnell WR, Perkins-Veazie P, Russo VM, Collins J, Seeland TM, Effects of deoxynivalenol on content of chloroplast pigments in barley leaf tissues, Phytopathology 100 (1) (2010) 33. [PubMed: 19968547]

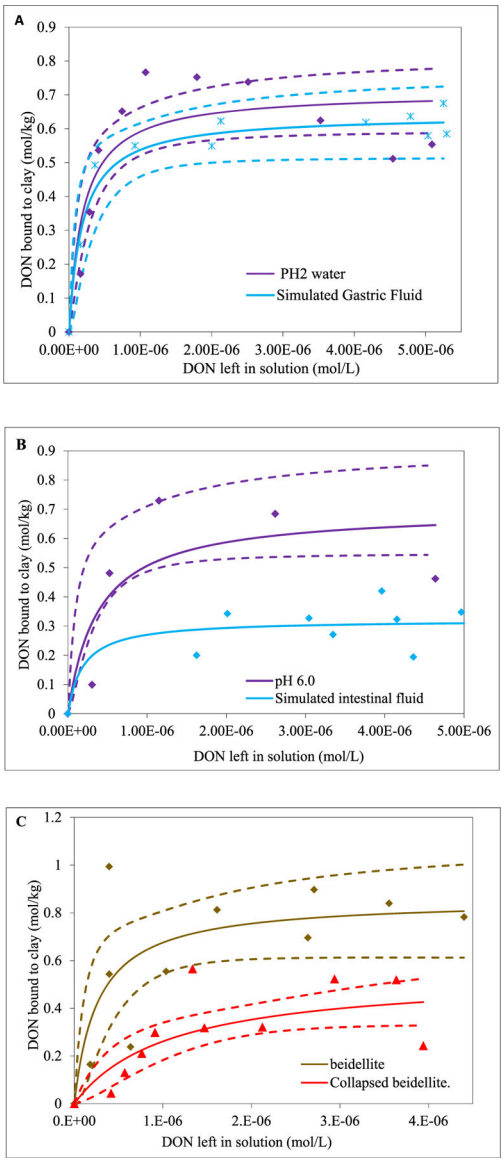

Fig. 1.

Adsorption isotherms of DON onto beidellite clay at 37 °C plotted by the Langmuir model at (A) pH 2, (B) pH 6, and (C) pH 2 with collapsed beidellite. Data represents the mean adsorption (mol/kg) at each concentration run in triplicate. Bands indicated 95 % confidence intervals on the mean response.

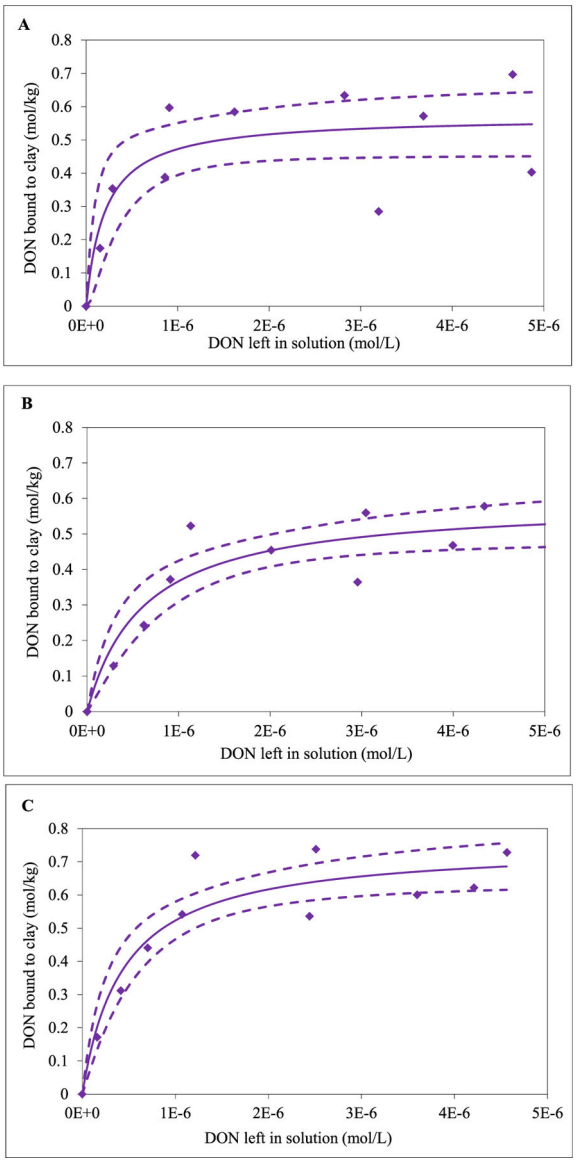

Fig. 2.

Adsorption isotherms of DON onto beidellite clay at pH 2 plotted by the Langmuir model at (A) 4 °C, (B) 18 °C, and (C) 37 °C. Data represents the mean adsorption (mol/kg) at each concentration run in triplicate. Bands indicated 95 % confidence intervals on the mean response.

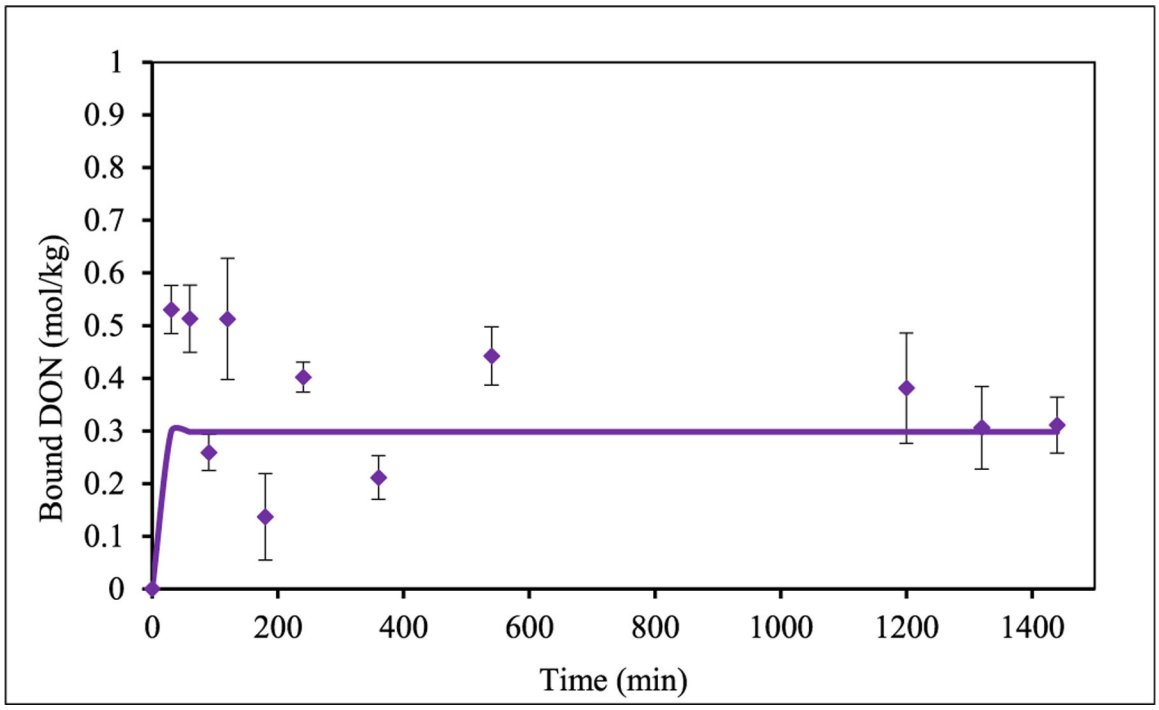

Fig. 3.
Time course of the adsorption of DON.

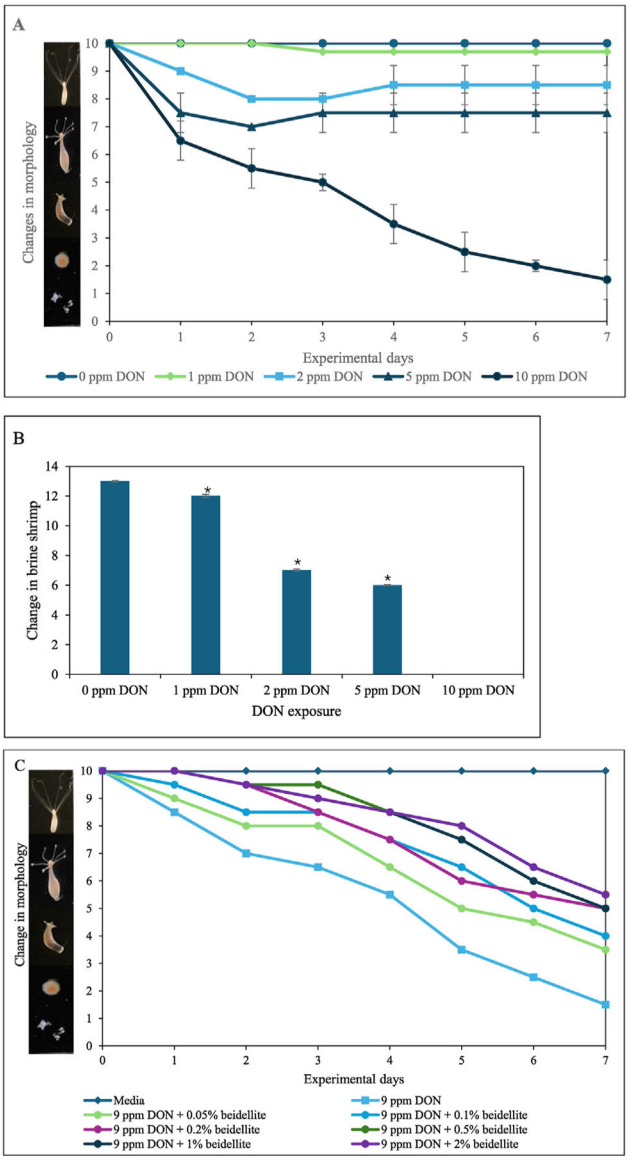

Fig. 4.

Toxicity of exposure to DON in (A) hydra morphology and, (B) feeding ability, (C) dose-response protection with beidellite clay. * indicates a significant difference ($p < 0.05$) compared to the vehicle control group. Data is presented as mean ± standard deviation, n = 3.

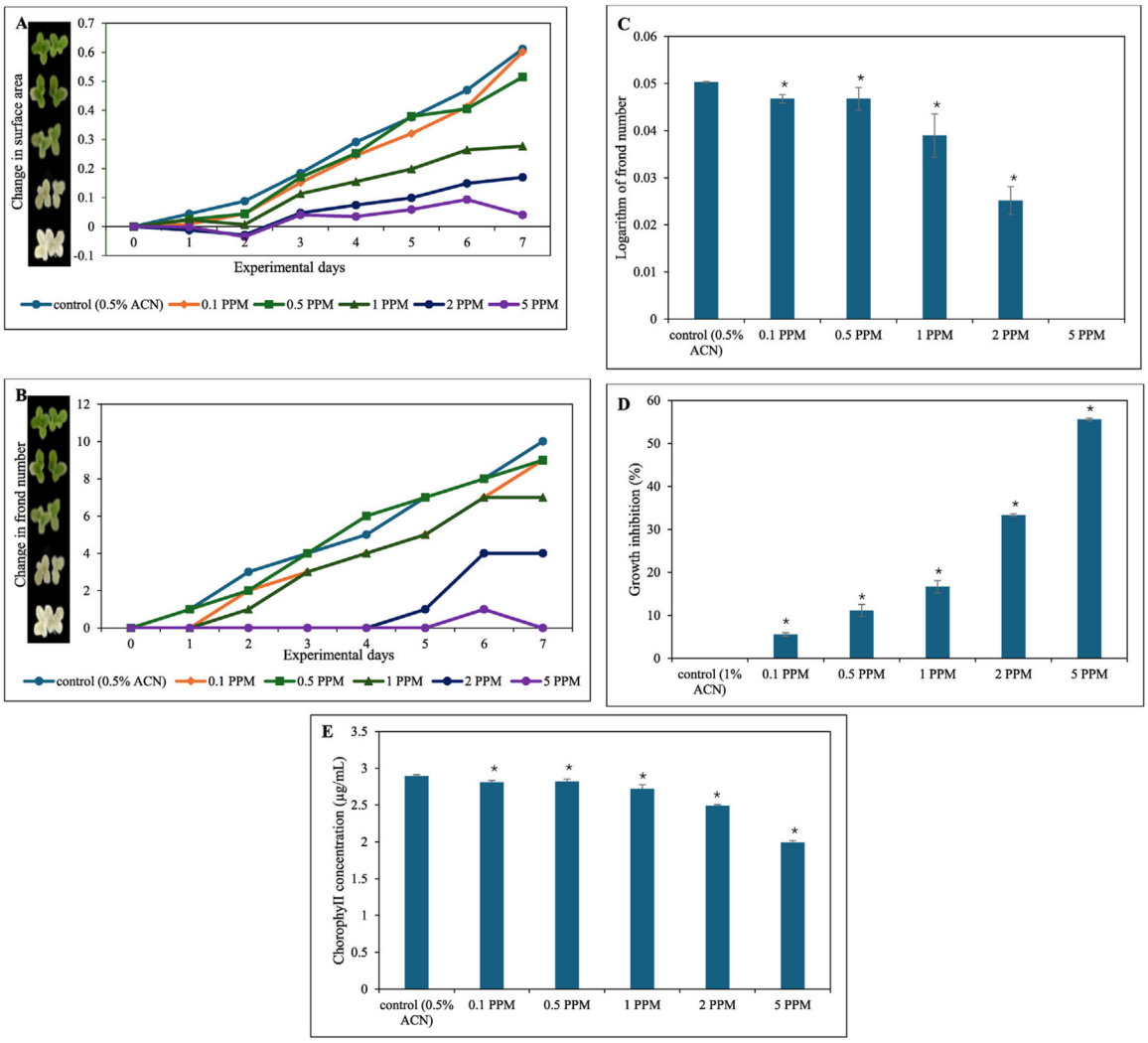

Fig. 5.

Toxicity of DON on *Lemna minor* in terms of (A) surface area, (B) frond number, (C) growth rate at day 7, (D) growth inhibition, and (E) chlorophyll content. * indicates a significant difference ($p < 0.05$) compared to the vehicle control group. Data is presented as mean ± standard deviation, n = 3.

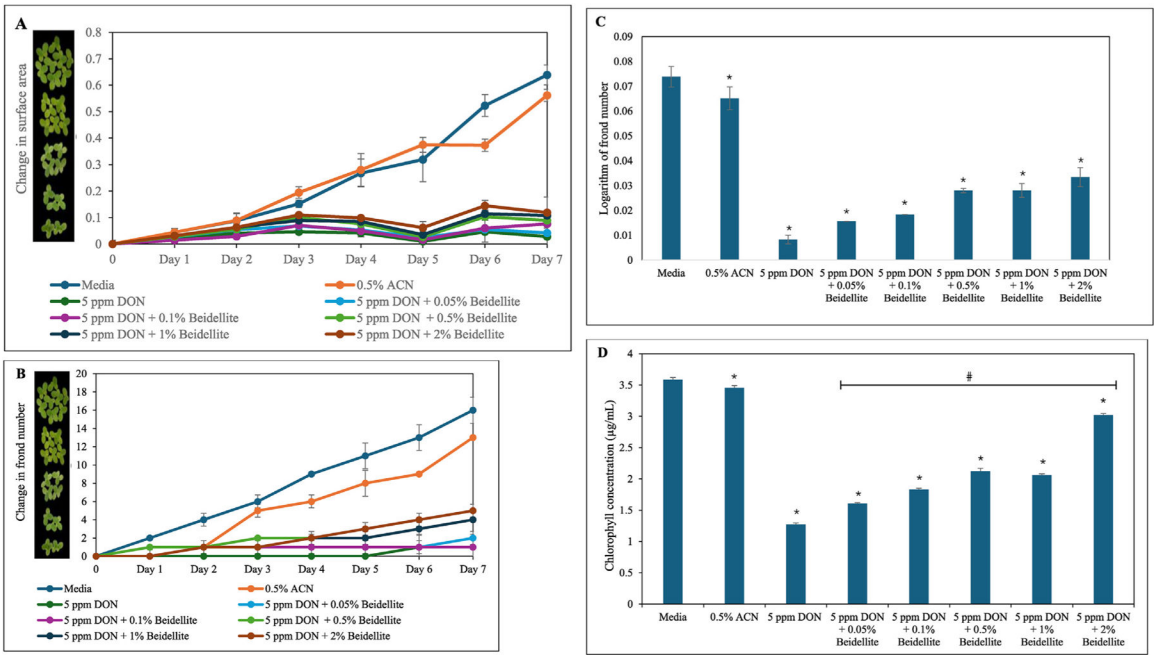

Fig. 6.

Dose-dependent protection by beidellite clay against DON toxicity on *Lemna minor* in terms of (A) surface area, (B) frond number, (C) growth rate at day 7, and (D) chlorophyll content. * indicates a significant difference ($p < 0.05$) compared to the vehicle control group. Data is presented as mean ± standard deviation, n = 3.

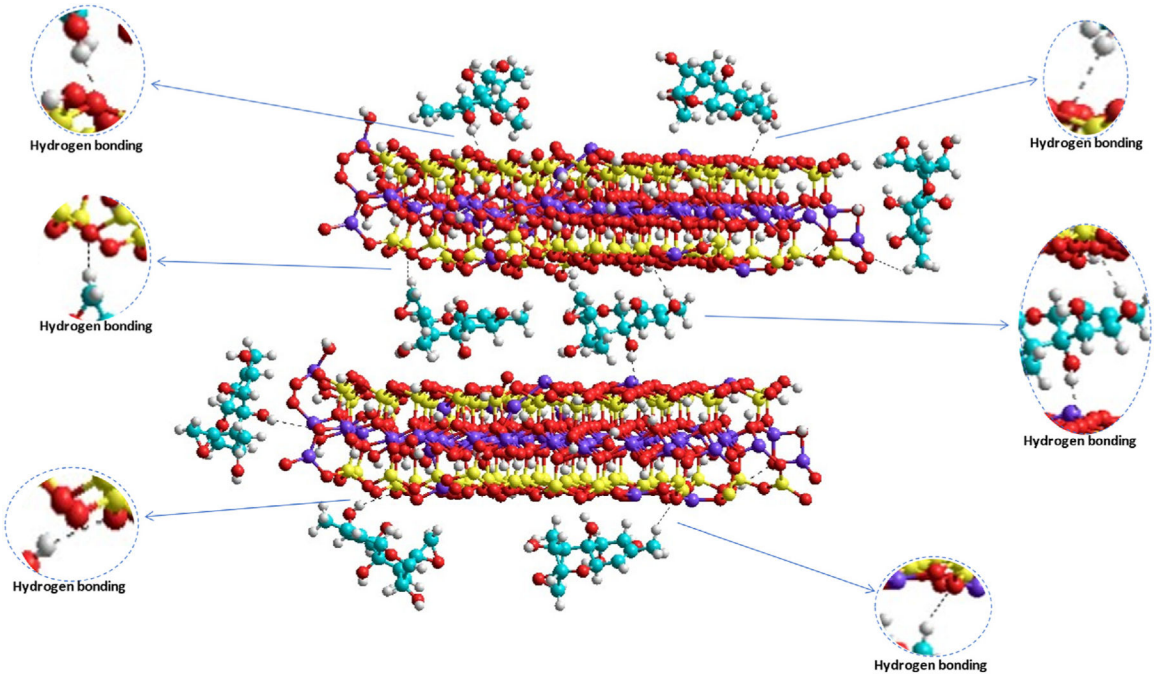

Fig. 7.

Energy minimized molecular model of DON binding onto simulated beidellite clay with close-up views of hydrogen bonding modes. Atom color code: Silicon (yellow), Carbon (cyan), Aluminum (violet), Oxygen (red), Hydrogen (white). Based on the chemical formula of beidellite, the tetrahedral surface Si^{4+} atoms were exchanged with Al^{3+} atoms at a ratio of 7:1 resulting in a higher charge distribution at the edges of the interlayer surfaces.

Table 1

Parameters and correlation coefficients of adsorption in the Langmuir model.

	Q_{max}	K_d	ΔG	r^2	MSE	ΔH
pH 2, 37 °C	0.75	2.28×10^6	−35.78	0.91	5.65×10^{-3}	
pH 6, 37 °C	0.70	2.63×10^6	−38.12	0.71	NA	
pH 2, 4 °C	0.57	4.82×10^6	−35.98	0.93	1.38×10^{-2}	−34.08
pH 2, 18 °C	0.59	1.63×10^6	−33.54	0.92	4.78×10^{-3}	
SGF, 37 °C	0.64	4.23×10^6	−30.27	0.92	7.92×10^{-2}	
SIF, 37 °C	0.40	9.77×10^5	−34.10	0.88	1.03×10^{-2}	

MSE: Mean squared error; r^2: correlation coefficient; ΔG: Gibbs free energy (kJ/mol); K_d: binding affinity; Q_{max}: binding capacity (mol/kg); ΔH: Enthalpy (kJ/mol); SGF: simulated gastric fluid; SIF: simulated gastrointestinal fluid.

Table 2

Adsorption kinetic parameters for DON on beidellite.

Kinetic model	Parameter	Beidellite
Pseudo-second-order	qe (exp mg kg^{-1})	0.37
	qe (cal mg kg^{-1})	0.21
	K^2	1.34×10^7
	r^2	0.96

qe (exp): binding at equilibrium in experiment; qe (cal): binding at equilibrium calculated by pseudo-second-order; K_2: rate constant of the second order; r^2: correlation coefficient.